Lawrence Berkeley National Laboratory

NUCLEAR COLLECTIVITY IN HIGHLY EXCITED STATES

Author
Diamond, R.M.

Publication Date
1981-10-01

MASTER

LBL-13723

CONF-8110157--1

Lawrence Berkeley Laboratory
UNIVERSITY OF CALIFORNIA

Presented at the Symposium on Nuclear Collectivity, Dogashima, Japan, October 14-16, 1981

NUCLEAR COLLECTIVITY IN HIGHLY EXCITED STATES

R.M. Diamond

October 1981

NUCLEAR SCIENCE DIVISION

Prepared for the U.S. Department of Energy under Contract W-7405-ENG-48

LBL-13723

Nuclear Collectivity in Highly Excited States

R.M. Diamond

Nuclear Science Division
Lawrence Berkeley Laboratory
University of California
Berkeley, CA 94720

DISCLAIMER

LBL--13723

DE82 007610

This work was supported by the Director, Office of Energy Research, Division of Nuclear Physics of the Office of High Energy and Nuclear Physics of the U.S. Department of Energy under Contract W-7405-ENG-48.

I would like to tell you about two recent studies we have done involving continuum γ-ray spectroscopy. Both are about highly excited states, and both involve collective motions, although of two different types. But before describing these experiments, I would like to take a few minutes to talk more generally about continuum spectra. This subject has become important because it is closely related to high-spin states.[1] At present our best, and almost only, source of information about such states comes from the study of the continuum spectra de-exciting these states. There are so many pathways down that none have enough intensity to be seen individually, and only after the population has condensed onto the yrast line and a few bands above it can discrete transitions be distinguished by our present-day detectors.

Figure 1 shows what a continuum spectrum from the $^{126}Te(^{40}Ar,4n)^{162}Yb$ reaction looks like.[2] The hollow squares are the raw pulse-height data from a 7.6 x 7.6 cm NaI detector in coincidence with a Ge(Li) detector. The NaI is placed 60 cm from the target so as to permit separation of neutrons and gammas by time-of-flight. The filled circles are the same data corrected for the detector response function and normalized to the number of transitions per 40 keV channel per event. The integral of this curve is then the average γ-ray multiplicity, the average number of transitions emitted in the de-excitation cascades, ∿24 in the present example. There are three components in the spectrum. Above ∿1.6 MeV there is an exponential tail whose angular distribution (shown at the top of the figure) is roughly isotropic and whose conversion-electron spectrum (only one system studied twice[3,4]) suggests nearly pure E1 transitions. At the lower energy end, below ∿0.8 MeV, there are the discrete γ-ray lines of the ground band. And between these two components lie most of the continuum transitions, forming the "yrast bump".

In a well-deformed nucleus, such as this ^{162}Yb example, this region is composed predominantly of stretched E2 transitions as indicated by angular distribution[5-8] (see top of Fig. 1) and correlation measurements and by linear polarization experiments.[7-9]

How do these components fit into the general de-excitation pattern of an excited nucleus? Figure 2 shows a possible scheme. This is a plot of excitation energy vs spin for a doubly even compound nucleus. In a 170 MeV (^{40}Ar,xn) reaction, nuclei are created with a wide angular momentum distribution (0-70 ħ) and at ∿70 MeV of excitation energy. Neutrons are boiled off so as to cool the nucleus to within one neutron binding energy of the yrast line (the entry limit), and then γ-ray cascades remove the remaining excitation and the angular momentum. Two principal types of γ-ray transitions are indicated schematically in the figure. The "statistical" ones, represented by the statistical tail in Fig. 1 and probably mostly E1 transitions, carry off energy but little angular momentum (0 or 1 ħ) and so cool the nucleus towards the yrast line. But since they average 1.5-2.0 MeV, there can only be ∿4 of them. The more numerous "yrast-like" γ rays form collective bands roughly parallel to the yrast line; they are the stretched E2 transitions that carry off 2 ħ apiece. Several such γ-cascades are indicated in Fig. 2, but there are probably dozens or hundreds. In a strongly deformed nucleus, the decay may be down many such rotational bands to spins of 20-30 ħ before the statistical transitions and the band crossings can dump the population into the yrast line and a few bands above it so that individual transitions can be seen. In a near-spherical nucleus, the rotational bands are weaker so the nucleus may cool more quickly to the yrast line with the result that discrete yrast transitions can generally be seen to higher spin (30-40 ħ). Nevertheless, there are still many paths to that point; to learn about the higher states we must still study the preceding continuum γ rays.

I have suggested that the yrast-like bands are collective rotational ones. Is there experimental evidence to support this? The two most important characteristics of a rotational band are that 1) there is a definite relationship between the spin and energy of a state,

$$E = \frac{\hbar^2}{2\mathcal{J}} I(I + 1) \tag{1}$$

or for the γ-ray transition that is observed experimentally,

$$E_\gamma = \frac{\hbar^2}{2\mathcal{J}} (4I - 2) \tag{2}$$

and 2) the transitions are very much enhanced over single-particle ones.

There is not very much direct evidence on the collectivity of the yrast-like transitions, but some years ago a number of nuclei had the average feeding time from the start of the cascades down to spin 8 or 10 ħ in the ground band determined roughly in the course of Doppler-shift recoil-distance measurements of the lifetimes of states in the ground band.[10-15] These feeding times were of the order of picoseconds, and since there are 20 or more transitions in these cascades, this means average lifetimes of ∿0.1 picosecond. Since the average transition energy is just over an MeV, this corresponds roughly to an E2 enhancement of several tens. Recently, two measurements[16] by Doppler-shift attenuation have given better values for the average enhancement of the cascade transitions from approximately spin 50 to 30 ħ for nuclei such as $^{159,160}Er$; these are large, 170 ± 60 s.p.u., indicating a collectivity of the same order as in the ground band of these deformed nuclei. It remains, however, to be seen if this is generally true or only happens in this particular case.

The other main characteristic of rotational bands is the transition energy-spin relationship given by eq. (2). If this holds for the continuum cascades shown in Fig. 1, then the upper edge of the yrast bump at ~1.4 MeV corresponds to the highest energy rotational transitions from the highest spin states. If the total amount of angular momentum brought into the compound nucleus were reduced, then the spin at the top of the cascades would be lowered and the maximum transition energy should also be reduced. The bottom of Fig. 1 shows the spectrum from 181 MeV $^{40}Ar + ^{126}Te \rightarrow ^{162}Yb + 4n$ drawn in again schematically as a solid line, and the spectrum for a 157 MeV ^{40}Ar irradiation, corresponding to 12-13 ħ less angular momentum on average, is shown as a long-dashed line.[2] It can be seen that the statistical and the discrete γ-ray regions are little changed, but that the yrast bump region has mainly contributed to the decrease in average multiplicity (~6 transitions) and that its upper edge is ~300 keV lower in energy. That is, with a decrease in the average spin carried off by the γ-ray cascades from ~40 ħ to 27-28 ħ, the maximum γ-ray transition energy has decreased, in agreement with the behavior expected of a rotor, eq. (2). It might be noted that the two other curves drawn in Fig. 1 are for ^{162}Yb made with the same average angular momentum but by 87 MeV $^{16}O + ^{150}Sm$ and by 331 MeV $^{86}Kr + ^{80}Se$. The similarity in the three curves shows that the amount of angular momentum and not the projectile-target combination is all-important in determining the shape of the yrast-bump region.

If we now assume that rotational cascades do occur, we can turn the story around and use the energy of the bump edge and its corresponding spin (determined from the multiplicity) in order to solve for the effective moment of inertia from eq. (2). By changing the bombarding energy, another value can be obtained at a different spin region. This was the first experimental method for determining $\mathcal{J}_{eff}$ at high spin and gave values in agreement with those for a rigid sphere or a deformed liquid drop within the ~15% errors in the experimental and in the calculated values. More objective and better values can be obtained by using a multiplicity-filter technique and plotting multiplicity vs E_γ, or by using a sum spectrometer in coincidence with the detector sampling the spectrum. The problem with both of these types of measurements (and with most continuum determinations) is that one is observing an average value over a wide distribution in spin, of the order of 60% FWHM. The "crystal balls" (a 72-sector one is now operating at Oak Ridge, and a 162-sector one is nearing completion at the M.P.I., Heidelberg) will do better than this, yielding a 20-25% FWHM, but at the moment the sum spectrometer method probably provides the best results.

The idea is as follows. The target is surrounded as completely as possible by a large NaI detector so that 80-90% of the total γ-ray energy emitted by the reaction product is captured.[17] In pairwise coincidence with this total-energy detector are several smaller detectors at a greater distance from the target (to discriminate against neutrons), which sample the continuum spectrum with a small solid angle. In the analysis of the data one can produce continuum spectra that are in coincidence with different energy gates (slices) of the total-energy spectrum. For example, one can look at spectra in coincidence with the first 5 MeV slice of the total energy, the second 5 MeV slice, and so on. Such spectra are shown in the upper part of Fig. 3, where the numbers give the order of the sum slices and the vertical scale is the number of transitions per event per 200 keV channel in the γ-ray transition energy.[18] For the higher slices, the yrast bump appears and its upper edge moves to higher energy with higher total energy (higher average spin). This is most easily seen in the bottom part of the figure where the differences between consecutive spectra are shown. The centroid of such a difference peak gives a maximum transition energy for which the average of the multiplicities of the two spectra involved gives a measure of the corresponding spin. Thus, a value for the effective moment of inertia can be calculated for the centroid of each difference peak. The result of a recent set of such measurements from 185 MeV ^{40}Ar + ^{124}Sn to yield predominantly ^{159}Er is shown in Fig. 4 as open circles[19] on the usual backbend plot of $2\mathcal{J}/\hbar^2$ vs $(\hbar\omega)^2$ ($\hbar\omega = E_\gamma/2$). Also shown are the values of $2\mathcal{J}/\hbar^2$ obtained for the discrete yrast transitions of ^{158}Er up to spin 36 $\hbar$ (filled circles) and the predictions of the liquid-drop model (dashed curve). A rigid rotor would give a horizontal line. The points for ^{158}Er rise initially because of the Coriolis anti-pairing effect, the decrease in the pairing correlations for all nucleons. At spin 14 $\hbar$ there is the first band-crossing and consequent large backbending. The crossing band is a 2-quasiparticle band with two unpaired and aligned $i_{13/2}$ neutrons contributing $\sim$10 $\hbar$ to the total angular momentum. At spin 28 $\hbar$ there is a second band-crossing, this time by a 4-quasiparticle band (two additional $h_{11/2}$ protons, most probably), giving a smaller upbend involving perhaps 6 $\hbar$ of additional aligned angular momentum. Our effective moments of inertia derived from the continuum spectra of $^{159,160}Er$ just overlap the end of the transition energy region of the discrete values in ^{158}Er, but it should be noted that there is a ±10% uncertainty in the absolute values of the former. The relative errors in the values given by the hollow circles are smaller, however, of the order of 3-4%, so that we believe that the upturn at the high-ω end is real. In fact, the actual effect is probably larger and likely occurs at a higher transition energy but is smeared out by our poor spin resolution.

We do not know the origin of this upturn around spin 50 $\hbar$, but theoretical calculations suggest a possible explanation. For nuclei around $Z = 65$ and $N = 82$-86, these calculations indicate a significant shell effect,[20] an energy-level gap, at high spin for prolate nuclei with principal axes in the ratio of 2:1. That is, a nucleus of lower deformation in this region of N, Z, and spin would go to a lower energy state by deforming to such a 2:1 shape. The result, of course, would be an increase in $\mathcal{J}$ and a decrease in the energy of rotational transitions in such a nucleus. This is not as exotic a suggestion as it might first appear. Such a shell effect is predicted, and does occur, in the ground state of nuclei around $Z = 95$. It causes the second minimum in the potential barrier leading to the spontaneously fissioning isomers[21] observed in a number of Pu and Am nuclei, and measurement of their rotational energy-level spacings and quadrupole moment does indicate a 2:1 axis ratio.[22] If this shell-effect explanation is correct for the present situation also, then it should vanish for nuclei of higher mass and should occur more strongly for slightly lighter nuclei in the $N = 82$-86, $Z = 65$ region, and then disappears again for still smaller nuclei. Only future experiments will give us the answer to these questions.

Now I would like to shift to another group of experiments that are quite recent; we started them at the end of last year. They involve the observation of giant dipole resonance (GDR) decay from highly excited states in nuclei, and by the time I finish I hope you will appreciate why our group is excited about the possibilities of these experiments. The GDR, the vibration of the neutrons against the protons in a nucleus, was the first collective motion studied.[23-25] Excitation of the resonance based on the ground state has been observed in many nuclei, and its systematics has been studied, both theoretically and experimentally, with quite reasonable agreement. However, Brink has proposed[26] that every state in a nucleus, not just the ground state, has a GDR based on it. And in several light nuclei, excitation of the GDR based on the first excited state has been observed.[27] But a possible corollary to Brink's hypothesis is that many states more than 15-20 MeV above the yrast line would have the possibility of E1 decay with a Lorentzian-like strength function and with a magnitude given by the E1 sum rule. Such a variation with E_γ would result in an enhanced probability of continuum γ-ray transitions near the GDR energy, ~15 MeV. In fact, enhancement of the region from 8-20 MeV in the γ-ray spectrum following the spontaneous fission of ^{252}Cf has been observed and ascribed to GD decays,[28] and we have now observed this effect in the continuum γ-ray spectrum following heavy-ion fusion[29] and deep inelastic reactions.

Three examples of the high energy part of the γ-ray spectrum observed in eight 12.7 x 15.2 cm NaI detectors placed 50 cm from the target and in coincidence with a sum spectrometer are shown in Fig. 5. The sum spectrometer had eight sectors, and events were stored only if more than six of these gave coincident pulses. Beams of 5-10 ena of 170 MeV ^{40}Ar from the LBL 88" cyclotron were used to bombard ~1 mg/cm^2 targets ranging from ^{27}Al to ^{124}Sn. For the region $2 \leq E_\gamma \leq 8$ MeV, the spectrum for each target shows an exponentially falling tail, the statistical transitions. All spectra rise above this exponential line at energies above ~10 MeV, suggesting a new component of γ rays. Above ~20 MeV the spectra are low and flat, probably due to cosmic rays. The reason for the initial steep slopes in the figure is that the transition probabilities are proportional to the ratios of the level density for the final states over that of the initial state, and these level densities vary approximately exponentially with E_x, the energy above the yrast line. Thus, the transition probabilities depend on $\exp(-E_\gamma/T)$. So a rough way to see the shape of the γ-ray strength functions is to remove the level density dependence by multiplying by $\exp(-E_\gamma/T_e)$, where T_e is an effective T. For $2 < E_\gamma < 8$ MeV, $T_e \approx 1$ MeV, whereas above 10 MeV the curves are flatter, indicating that these γ rays are emitted at a higher T_e. We have somewhat arbitrarily taken $T_e = 1.43$ MeV for the ^{164}Er compound nucleus (^{124}Sn target), and adjusted the others for the expected mass dependence, $T \propto A^{-1/2}$. The same data from Fig. 5 (with the flat high-energy background subtracted) multiplied by these exponentials are shown in Fig. 6. Peaks are now visible that have maxima (~14 MeV) and widths similar to those for the GDR based on the ground state. They go up in energy as the target mass decreases, as is expected for the GDR ($E_G \sim A^{-1/3}$). Integrating the original spectra between 10 and 20 MeV gives 2-3 x 10^{-3} transitions per cascade for all three targets.

These results may be compared with calculations using the computer code GROGI2;[30] Fig. 7a shows the calculated γ-ray spectrum for the ^{164}Er system. The dashed line is for a constant E1 matrix element, while the full curve is for a strength function involving a Lorentzian-like shape with a maximum at 15 MeV and a width of 5 MeV. It can be seen that even with the constant E1 matrix element there is a noticeable change in slope around 8 MeV. This arises from the following feature. Approximating the level densities as $\rho(E_x) \propto \exp(E_x/T)$, where E_x is measured from the yrast line, the ratio of the probability of decay by an E1 γ ray of energy E_γ to the more probable decay by a neutron can be estimated by the ratio of the E1 width, $\Gamma_\gamma(E_\gamma)$, to the total neutron width, Γ_n, derived from the statistical model of nuclear decay,

$$\Gamma_\gamma(E_\gamma)/\Gamma_n \propto E_\gamma^3 f(E_\gamma) T^{-2}[\exp(B_n + 2KT - E_\gamma)/T] \qquad (3)$$

Here B_n and 2KT are the binding energy and average kinetic energy of the neutron. If $E_\gamma < (B_n + 2KT)$, as is usually the case, then Γ_γ/Γ_n decreases with increasing E_x. But when $E_\gamma > (B_n + 2KT)$, the exponential changes sign and the situation reverses, so that the branching ratio increases with increasing E_x. Thus, these high-energy transitions come preferentially from states of high excitation (high T) and so show a smaller slope than the low energy transitions.

If instead of a constant matrix element, the GDR strength function

$$f(E_\gamma) = K(NZ/A)\Gamma_G E\,[(E^2 - E_G^2)^2 + (E_\gamma \Gamma_G)^2]^{-1} \tag{4}$$

is used in GROGI2, the resulting spectrum (full line in Fig. 7a) is similar to the experimental one, and integration of the yield between 10 and 20 MeV gives 1.9×10^{-3} transitions per cascade, in good agreement with the observed value. Multiplying the spectrum by $\exp(E_\gamma/1.43)$ gives the spectrum shown in Fig. 7b. The dashed line here is the Lorentzian shape put into the calculation. The agreement suggests that the procedure used in Fig. 6 can indicate the shape of the strength functions involved and that the experimental results in Fig. 6 are compatible with Lorentzian-like functions rather than constant values. However, it is true that the calculated peak is considerably higher and sharper than the experimental one. Partly this is due to using a slightly too high value for E_G and a considerably too small value for Γ_G, but such problems will have to be considered in more detail in the future. One more comparison with simple theory can be made. From eq. (3) it has been argued that the yield of high energy γ rays per event should increase with increase in excitation energy. Figure 8 shows the spectra from the de-excitation of the $^{122}Te^*$ compound nucleus taken in coincidence with a high, medium, and low cut on the sum spectrometer. This sequence corresponds to a low, medium, and high excitation energy above the yrast line, and it can be seen that the yield of ~14 MeV γ rays is about twice as high with the low sum cut (high excitation energy) as with the high sum cut (low excitation energy), in agreement with expectation.

It seems most likely that we are seeing GDR γ rays emitted from the highly excited compound states in competition with neutron (or other particle) evaporation. If true, a most exciting prospect is to look for structure in the resonance peak. For if the nucleus is deformed into an axially symmetric shape, the peak will split in two. If the deformation is prolate, the lower energy component will have 1/3 the total intensity and the higher one 2/3, and the inverse will be true if the nucleus is oblate. If it is triaxial, the GDR peak will split into three components. Furthermore, if such structure exists, there will be a difference in the angular distribution of the different parts. If either the structure or the angular distribution, or both, can be observed, we shall be able to determine the shape of nuclei at high spin and excitation energy and in a way that should be quite general for many nuclei.

As I hope you have seen, the field of continuum γ-ray spectroscopy is a rapidly developing and changing one, and the introduction of new experimental techniques such as the use of crystal-ball, 4π detector systems can only accelerate the pace. I should also note that theoretical developments are also proceeding along similarly expanding lines, so that we may look forward to a wealth of new information on high spin and highly excited states in the next few years and much more detailed knowledge about their structure.

Acknowledgements

I would like to thank all the group of very able and congenial visitors and collaborators who have contributed so much to the many helpful discussions and to the continuum γ-ray experiments of the last few years. That list would be too long, so I shall mention only those involved during the last year: O. Andersen, M.A. Deleplanque, E.L. Dines, J.E. Draper, C. Ellegaard, Y. Ellis-Akovali, J. Garrett, B. Herskind, D. Lebeck, M.K. Lee, K.H. Lindenberger, J.O. Newton, S. Newton, C. Schück, S. Shih, and particularly my partner, F.S. Stephens. This work was supported by the Director, Office of Energy Research, Division of Nuclear Physics of the Office of High Energy and Nuclear Physics of the U.S. Department of Energy under Contract W-7405-ENG-48.

References

1. R.M. Diamond and F.S. Stephens, Annual Review of Nuclear and Particle Science (Annual Review, Inc., Palo Alto, CA) 1980, p. 85
2. R.S. Simon, M.V. Banaschik, R.M. Diamond, J.O. Newton, and F.S. Stephens, Nucl. Phys. A290, 253 (1977)
3. L. Westerberg, D.G. Sarantites, K. Geoffrey, R.A. Dayras, J.R. Beene, M.L. Halbert, D.C. Hensley, and J.H. Barker, Phys. Rev. Lett. 41, 99 (1978)
4. S.J. Feenstra, J. Van Klinken, J.P. Pijn, R. Janssens, C. Michel, J. Steyaert, J. Vervier, K. Cornelis, M. Huyse, and G. Lhersonneau, Phys. Lett. 80B, 183 (1979)
5. R.S. Simon, R.M. Diamond, Y. El Masri, J.O. Newton, P. Sawa, and F.S. Stephens, Nucl. Phys. A313, 209 (1979)
6. M.A. Deleplanque, T. Byrski, R.M. Diamond, H. Hübel, F.S. Stephens, B. Herskind, and R. Bauer, Phys. Rev. Lett. 41, 1105 (1978)

7. J.P. Vivien, Y. Schutz, F.A. Beck, E. Bozek, T. Byrski, C. Gehringer, and J.C. Merdinger, Phys. Lett. 85B, 325 (1979)

8. W. Trautmann, J.F. Sharpey-Schafer, H.R. Andrews, B. Haas, O. Häusser, P. Taras, and D. Ward, Phys. Rev. Lett. 43, 991 (1979)

9. H. Hübel, R.M. Diamond, F.S. Stephens, B. Herskind, and R. Bauer, Z. Phys. A297, 237 (1980)

10. R.M. Diamond, F.S. Stephens, W.H. Kelly, and D. Ward, Phys. Rev. Lett. 22, 546 (1969)

11. W. Kutschera, D. Dehnhardt, O.C. Kistner, P. Kump, B. Povh, H.J. Sann, Phys. Rev. C5, 1658 (1972).

12. J.O. Newton, F.S. Stephens, and R.M. Diamond, Nucl. Phys. A210, 19 (1973)

13. D. Ward, H.R. Andrews, J.S. Geiger, R.L. Graham, Phys. Rev. Lett. 30, 493 (1973)

14. N. Rud, D. Ward, H.R. Andrews, R.L. Graham, J.S. Geiger, Phys. Rev. Lett. 31, 1421 (1973)

15. B. Bochev, S.A. Karamyan, T. Kutsarova, V.G. Subbotin, Sov. J. Nucl. Phys. 22, 343 (1975)

16. H. Hübel, U. Smilansky, R.M. Diamond, F.S. Stephens, and B. Herskind, Phys. Rev. Lett. 41, 791 (1978)

17. P.O. Tjøm, I. Espe, G.B. Hagemann, B. Herskind, and D.L. Hillis, Phys. Lett. 72B, 439 (1978).

18. H.J. Körner, D.L. Hillis, C.P. Roulet, P. Aguer, C. Ellegaard, D.B. Fossan, D. Habs, M. Neiman, F.S. Stephens, and R.M. Diamond, Phys. Rev. Lett. 43, 490 (1979)

19. F.S. Stephens, et al., to be published.

20. G. Leander, C.G. Andersson, S.G. Nilsson, I. Ragnarsson, S. Aberg, J. Almberger, T. Døssing, and K. Neergaard, Proc. Symposium on High-Spin Phenomena in Nuclei, ANL/PHY-79-4, p. 197, Argonne, Ill.

21. S.M. Polikanov, V.A. Druin, V.A. Karnaukhov, V.L. Mikheev, A.A. Pleve, N.K. Skobelov, V.G. Subbotin, G.M. Terakopyan, and V.A. Fomichev, Sov. Phys. JETP 15, 1016 (1962)

22. V. Metag, Proc. of the Int. Conf. on Nuclear Physics, Berkeley, California (North-Holland Publishing Co., Amsterdam) 1981, vol. 2, p. 271

23. G.C. Baldwin and G.S. Klaiber, Phys. Rev. 71, 3 (1947); Phys. Rev. 73, 156 (1947)

24. M. Goldhaber and E. Teller, Phys. Rev. 74, 1046 (1948)

25. H. Steinwedel and J.H.D. Jensen, Z. Naturforsch. 5a, 413 (1950)

26. D.M. Brink, doctoral thesis, University of Oxford, 1955

27. P.P. Singh, R.E. Segal, L. Meyer-Schutzmeister, S.S. Hanna, and R.G. Allas, Nucl. Phys. 65, 577 (1965)

28. F.S. Dietrich, J.C. Browne, W.J. O'Connell, and M.J. Kay, Phys. Rev. C10, 795 (1974)

29. J.O. Newton, B. Herskind, R.M. Diamond, E.L. Dines, J.E. Draper, K.H. Lindenberger, S. Shih, C. Schück, and F.S. Stephens, Phys. Rev. Lett. 46 (1981)

30. J. Gilat, Brookhaven National Laboratory Report No. BNL 50246, 1970 (unpublished)

Figure Captions

Fig 1. Pulse-height (hollow squares) and unfolded (black dots) γ-ray spectra taken with NaI detectors in coincidence with a Ge(Li) counter for the reaction $^{126}Te(^{40}Ar,4n)^{162}Yb$ at 181 MeV. The larger dots are averaged over five channels. At the top is the 0°/90° ratio for the unfolded spectra. At the bottom are schematic unfolded spectra for the same case (solid line), for the same system but at 157 MeV (longer dashed line), for $^{80}Se(^{86}Kr,4n)^{162}Yb$ at 331 MeV (dotted line), and for $^{150}Sm(^{16}O,4n)^{162}Yb$ at 87 MeV (shorter dashed line). From reference 2.

Fig. 2. Typical γ-ray de-excitation pathways to the ground state for a deformed nucleus. The vertical arrows represent the statistical (cooling) transitions, whereas the yrast-like (rotational) transitions remove most of the angular momentum of the system.

Fig. 3. (top) Spectra from a 7.6 x 7.6 cm NaI detector corrected for the detector response function (number of transitions per 200 keV per event) for consecutive ~4 MeV wide slices of the coincident total γ-ray energy spectrum taken with a 33 x 20 cm sum crystal for the reaction products (mainly $^{159,160}Er$) of 185 MeV $^{40}Ar + ^{124}Sn$ $^{164}Er^*$ (ref. 18).

(bottom) The difference in spectra from consecutive slices as indicated in the figure.

Fig. 4. Plot of $2\mathcal{I}/\hbar^2$ vs. $(\hbar\omega)^2$ for the products (mainly $^{159,160}Er$) of the reaction 185 MeV $^{40}Ar + ^{124}Sn \rightarrow ^{164}Er^*$. The solid circles are the known transitions in ^{158}Er. The open circles are calculated from difference spectra like Fig. 3 as described in the text. The liquid-drop prediction is given by the dashed line.

Fig. 5. De-excitation γ-ray spectra from the indicated reactions taken with 12.7 x 15.2 cm NaI detectors in coincidence with a γ-ray total-energy NaI spectrometer. The shapes of the true γ-ray spectra are not expected to differ greatly from these, and so the ordinate in "transitions per MeV per cascade" should be approximately correct.

Fig. 6. Spectra of Fig. 5 with background subtracted and then multiplied by exp (E_γ/T_e) with T_e indicated on the figure. Arrows indicate $E_G = 78/A^{1/3}$ MeV, the centroid of the ground state GDR (ref. 29).

Fig. 7. (a) Gamma spectra for $^{164}Er^*$ from a GROGI2 calculation with a constant E1 matrix element---, with a Lorentzian-like strength function——.

(b) Giant resonance spectrum from (a) multiplied by exp $(E_\gamma/1.43)$. The dashed line is the Lorentzian function put into the calculation (see text) (ref. 29).

Fig. 8. De-excitation γ-ray spectra from the reaction $^{82}Se + ^{40}Ar \rightarrow ^{122}Te^*$ taken with 12.7 x 15.2 cm NaI detectors in coincidence with a γ-ray total-energy NaI spectrometer. Shown are spectra in coincidence with cuts on the low, medium, and high energy parts of the sum spectrum, as well as the sum of these spectra (ref. 29).

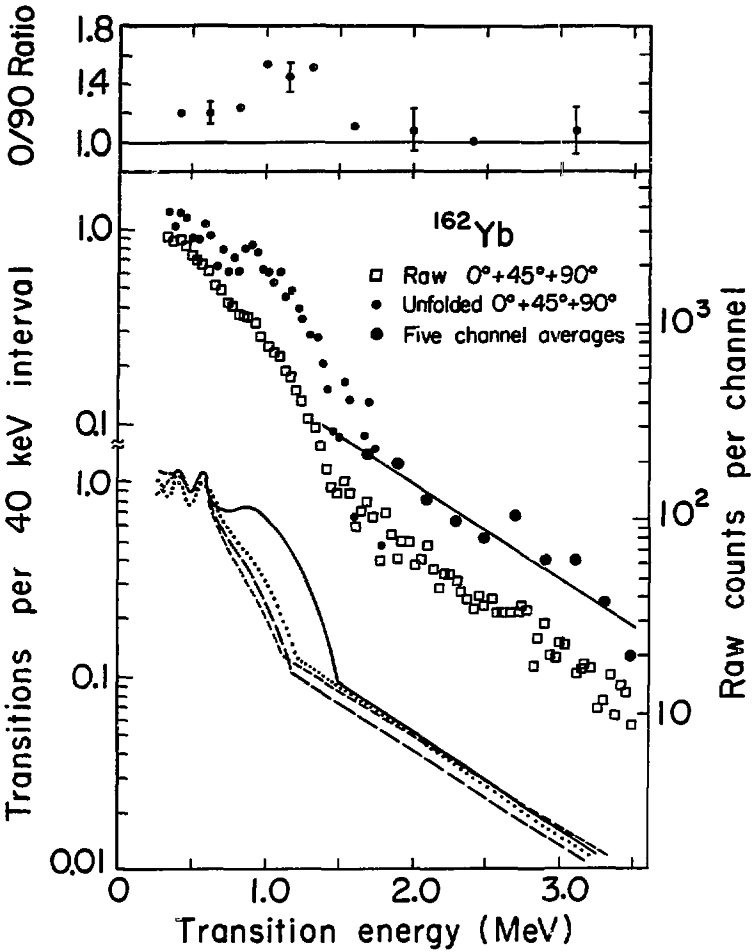

Fig. 1

XBL 771-162A

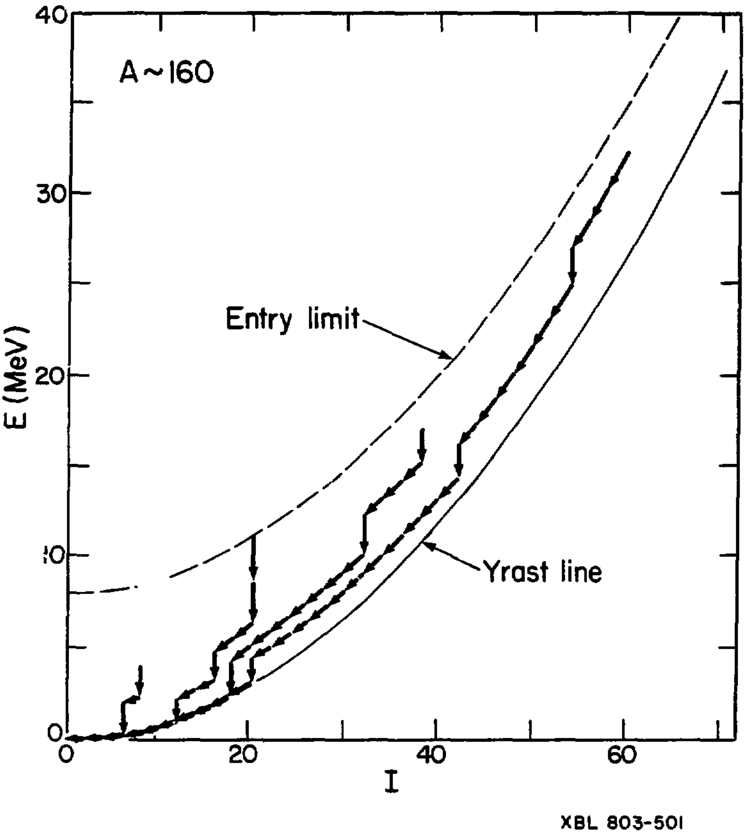
A~160
Entry limit
Yrast line
E (MeV)
I
0
10
20
30
40
0
20
40
60
XBL 803-501

Fig. 2

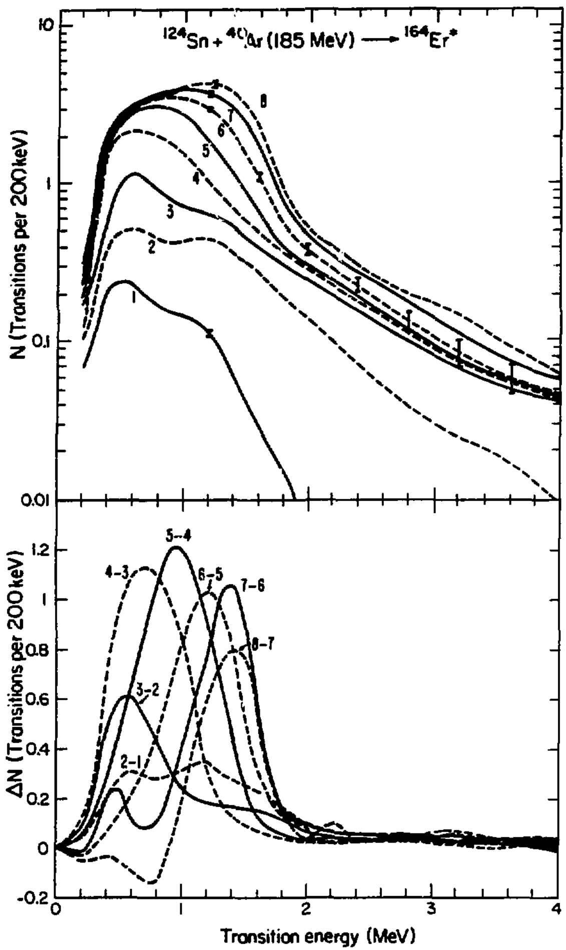

XBL 792-645A

Fig. 3

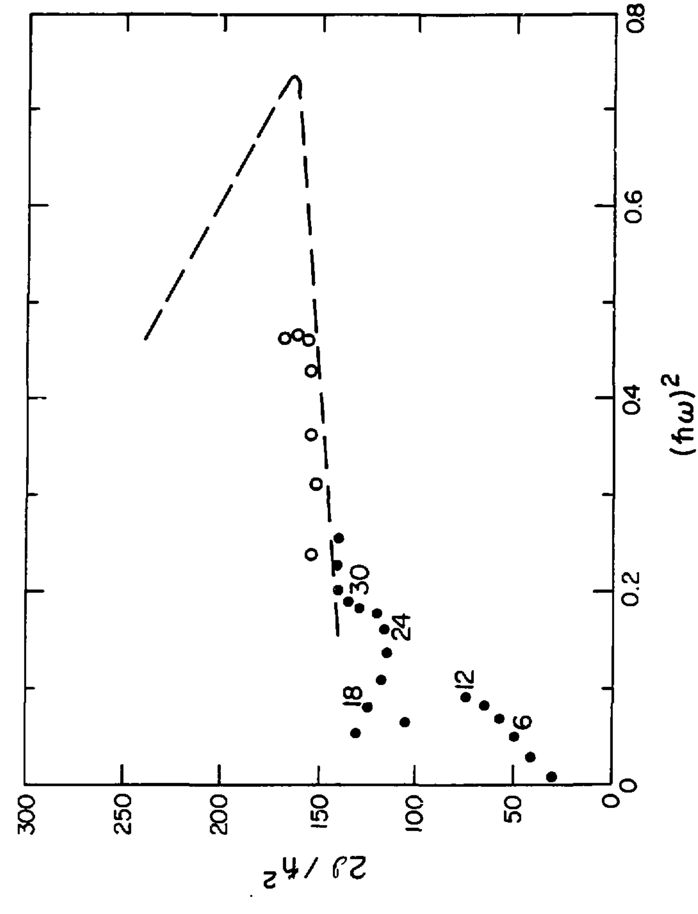

XBL 815-2297

Fig. 4

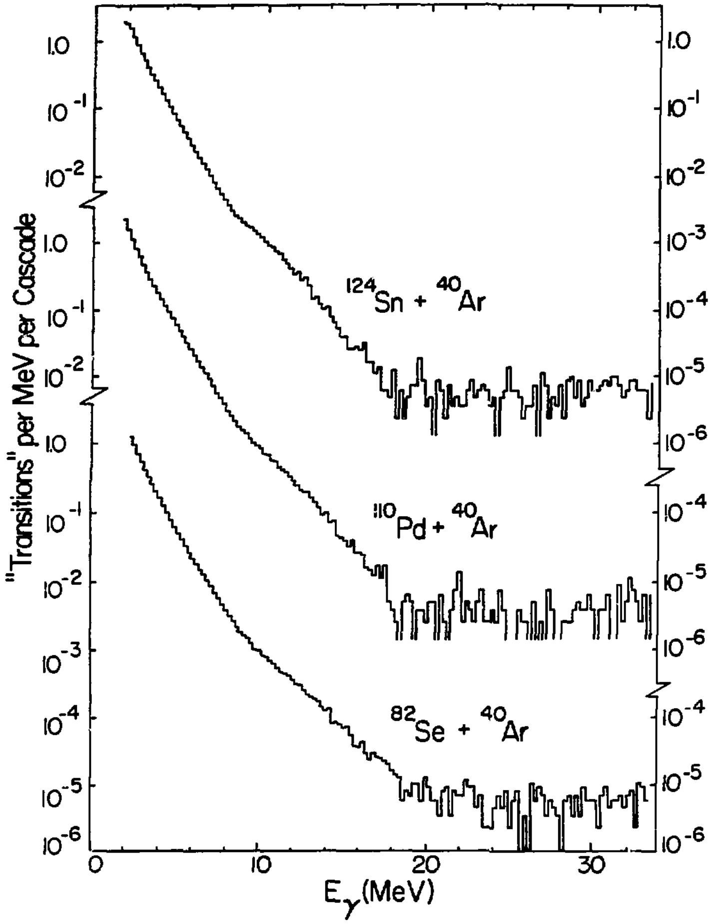

1.0
10^-1
10^-2
1.0
10^-1
10^-2
1.0
10^-1
10^-2
10^-3
10^-4
10^-5
10^-6
"Transitions" per MeV per Cascade
1.0
10^-1
10^-2
10^-3
10^-4
10^-5
10^-6
10^-4
10^-5
10^-6
10^-4
10^-5
10^-6
124Sn + 40Ar
110Pd + 40Ar
82Se + 40Ar
0
10
20
30
Eγ(MeV)
XBL 811-69

Fig. 5

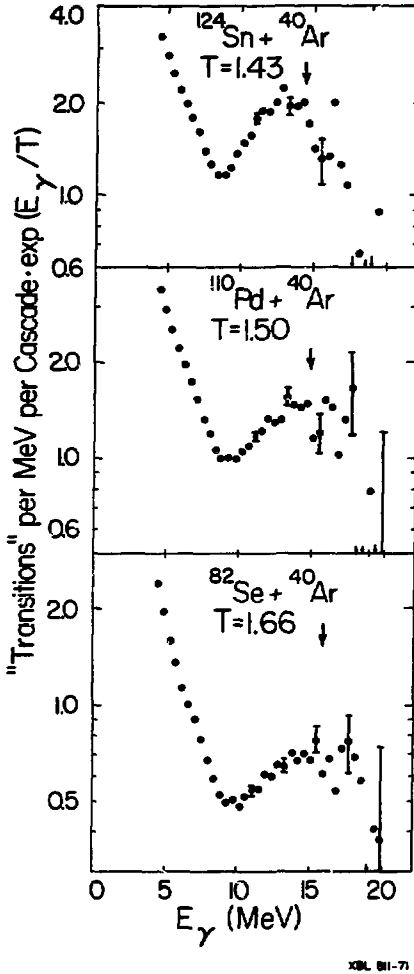
4.0
^{124}Sn + ^{40}Ar
T=1.43
2.0
1.0
0.6
^{110}Pd + ^{40}Ar
T=1.50
2.0
1.0
0.6
^{82}Se + ^{40}Ar
T=1.66
2.0
1.0
0.5
0
5
10
15
20
E_γ (MeV)
"Transitions" per MeV per Cascade·exp (E_γ/T)
XBL 811-71

Fig. 6

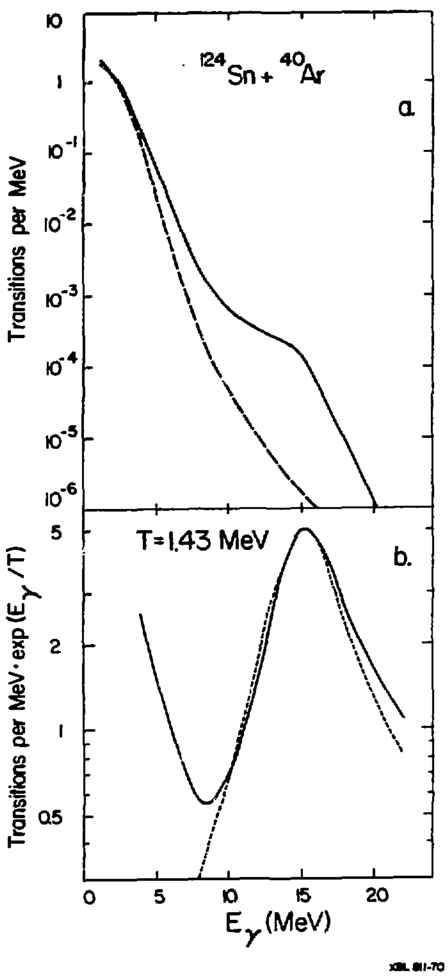

124Sn + 40Ar
a.
Transitions per MeV
10
1
10-1
10-2
10-3
10-4
10-5
10-6
T=1.43 MeV
b.
Transitions per MeV · exp (Eγ /T)
5
2
1
0.5
0
5
10
15
20
Eγ (MeV)
XBL 811-70

Fig. 7

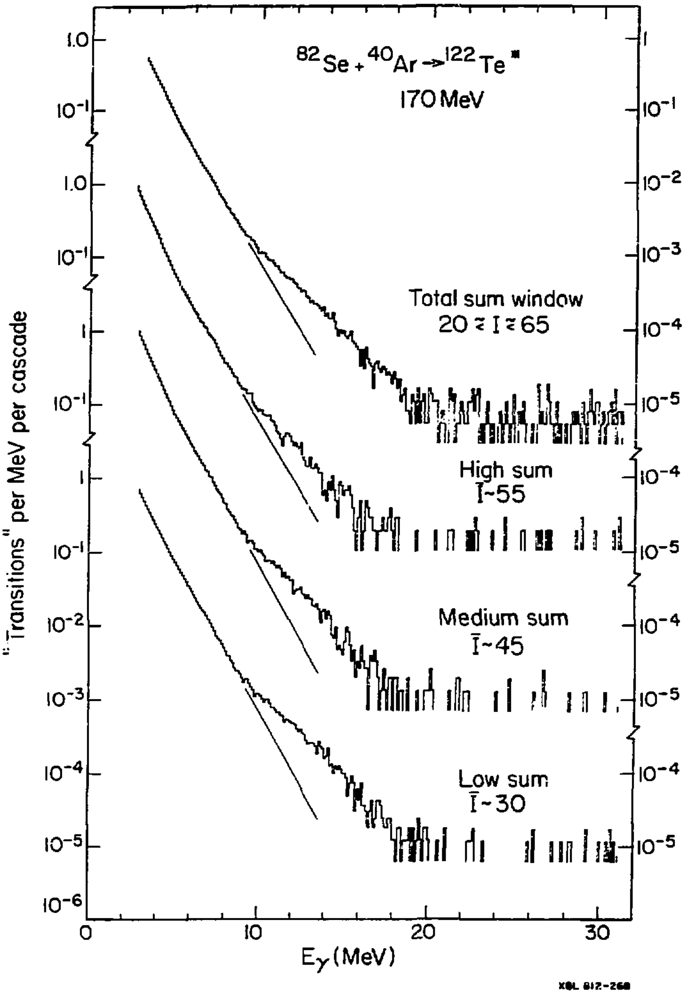

$^{82}Se + ^{40}Ar \rightarrow ^{122}Te^*$
170 MeV
Total sum window
20 ≲ I ≲ 65
High sum
Ī~55
Medium sum
Ī~45
Low sum
Ī~30
"Transitions" per MeV per cascade
Eγ (MeV)
XBL 812-268

Fig. 8